



Published in final edited form as:

Curr Biol. 2017 October 09; 27(19): 2901–2914.e2. doi:10.1016/j.cub.2017.08.035.

***Drosophila* spatio-temporally integrates visual signals to control saccades**

Jean-Michel Mongeau^{1,2} and Mark A. Frye^{1,*}

¹Department of Integrative Biology and Physiology, University of California - Los Angeles, Los Angeles, CA 90095-7239

SUMMARY

Like many visually active animals including humans, flies generate both smooth and rapid, saccadic movements to stabilize their visual gaze. How rapid body saccades and smooth movement interact for simultaneous object pursuit and gaze stabilization is not understood. We directly observed these interactions in magnetically-tethered *Drosophila* free to rotate about the yaw axis. A moving bar elicited sustained bouts of saccades following the bar, with surprisingly little smooth movement. By contrast, a moving panorama elicited robust smooth movement interspersed with occasional optomotor saccades. The amplitude, angular velocity, and torque transients of bar-fixation saccades were finely tuned to the speed of bar motion, and were triggered by a threshold in the temporal integral of the bar error angle, rather than its absolute retinal position error. Optomotor saccades were tuned to the dynamics of panoramic image motion, and were triggered by a threshold in the integral of velocity over time. A hybrid control model based on integrated motion cues simulates saccade trigger and dynamics. We propose a novel algorithm for tuning fixation saccades in flies.

Keywords

Flies; motion vision; feature detection; fixation; flight

INTRODUCTION

Humans generate body, head, and/or eye movements and saccades to fixate a moving visual object on the frontal fovea [1] whereas flies move their whole body in flight for the same purposes [2]. It has been suggested that a control system sharing the control effort between smooth movement and saccades would provide a good solution for robust object fixation in both arthropods and humans [3]. Flies robustly fixate an elongated vertical bar in free flight

*Lead contact

²Present address: Department of Mechanical and Nuclear Engineering, Pennsylvania State University, University Park, PA 16802

Publisher's Disclaimer: This is a PDF file of an unedited manuscript that has been accepted for publication. As a service to our customers we are providing this early version of the manuscript. The manuscript will undergo copyediting, typesetting, and review of the resulting proof before it is published in its final citable form. Please note that during the production process errors may be discovered which could affect the content, and all legal disclaimers that apply to the journal pertain.

AUTHOR CONTRIBUTIONS

JMM and MAF designed the study. JMM conducted the experiments and analyzed the data. JMM and MAF wrote the paper.

[4]. Studies of bar fixation in flies have primarily focused on revealing the visual parameters, control strategies, and circuitry for smooth movement in tethered animals [4–8], yet body saccades account for at least 80% of total net change in heading during free flight [9]. In tethered *Drosophila* rapid modulation in wing kinematics and yaw torque resembling saccades [10–12] are evoked by complex features moving within the visual periphery [8], yet the functional role of saccades for visual fixation in flies is unclear.

In human vision, saccades are grouped into different classes based on their underlying trigger and dynamics. In humans reflexive saccades are triggered by the appearance or disappearance of an external stimulus whereas scanning saccades are triggered endogenously for exploration of the visual environment [13]. In flies, computational techniques applied to free flight saccades have revealed that the vast majority are due to external sensory causes, and are thereby reflexive in nature [14], evoked by visual expansion of an approaching object or surface [15, 16]. Once a saccade is triggered, visual motion appears to play no role in modulating its dynamics [17, 18], suggesting that they are ballistic, all-or-none events. In tethered flight, flies generate saccades in the absence of any visual motion, suggesting that endogenous processes may also evoke saccades [10, 19].

With respect to dynamics, human saccades have been categorized into exploratory and fixating micro-saccades based on their amplitudes [20]. In flies, free flight saccades have been characterized as stereotyped with some variation in amplitude, time, and speed [21, 22]. The structure of a stationary background influences saccade rate and amplitude in freely flying blowflies [23] but has little effect on saccade dynamics in *Drosophila* [15]. Magnetically- and thread-tethered flies also generate spontaneous saccades that vary in their dynamics, with gross changes in the luminance or spatial layout of the visual panorama having some influence on saccade dynamics [12, 17]. In several instances, saccade dynamics have been shown to be modulated by visual objects – for example in hoverflies when chasing other flies [2] and in *Drosophila* prior to landing on a post [9].

Whereas rapid body saccades in flies are thought to re-orient the animal, flies also produce continuous optomotor steering responses to external displacements of the visual panorama. The underlying operation and mechanism of smooth optomotor movement in flies, which serves to reduce retinal slip and stabilize visual gaze against unintended course deviations, has been studied extensively [6, 11, 24, 25], as has the interplay between smooth optomotor movement and saccades for gaze control been the subject of several studies under free flight conditions [9, 26, 27]. Whether flies, like humans, dynamically tune saccade commands for object fixation or optomotor tracking remains unknown.

Here we examined the saccadic component of yaw-based visual fixation as well as the switch between saccadic and smooth flight optomotor movements. We used a magnetic tether apparatus in which a fly was tethered to a pin and suspended in a magnetic field [10, 28] and allowed to steer freely in yaw. The magnetic tether was surrounded by a cylindrical array of light emitting diodes (LEDs) that projected a panoramic background pattern superposed with a narrow vertical bar. Rotating the bar around the arena elicited robust tracking by the fly as it reflexively fixated it. Remarkably, bar fixation behavior is saccadic, with little smooth movement between saccades. By contrast, rotation of the textured

panorama in the direction opposite to the bar elicited smooth movement in between bar-fixation saccades. Prior work had established that saccades were evoked by a bar positioned within the visual periphery [5, 8]. We go substantially further to demonstrate that these saccades are triggered not by a threshold in absolute retinal position, but rather by a threshold in the temporal integral over space between the bar position and visual midline. For bars were moving fast, saccades were produced with more yaw torque than for bars moving slowly. Similarly, optomotor saccades were triggered by a threshold in the temporal integral of retinal slip. If the visual surroundings were moving simultaneously, saccadic bar fixation was unaffected [29], but flies immediately engaged smooth compensatory movement between every saccade. We propose a novel hybrid control model based upon spatio-temporal integration of visual signals.

RESULTS

Visual bar fixation is enabled by body saccades

Flies were tethered to a magnetic pin, and suspended in a free-yaw pivot tether (Figure 1A). We tested the hypothesis that flies rely on both smooth and saccadic movement when fixating a moving visual bar in yaw. Here the feature that distinguishes a “bar” is its motion relative to the surrounding visual panorama. We rotated a high-contrast, randomly-textured vertical bar over a similarly textured stationary background and measured flies’ heading angle as they attempted to fixate the bar. To our surprise, body saccades dominated visual fixation behavior (Figure 1B), with little smooth movement between saccades (Figure 1C, F) (Movie S1). Flies could continuously generate saccades directed towards the moving bar for several revolutions around the arena (Movie S1). The constantly revolving bar generally preceded the fly, such that the bar was fixated in the fronto-lateral field of view, rather than being centered on midline (Figure 1D, E). The full-width half-maximum of the distribution of the bar image on the retina was similar for a textured bar set against a similarly textured static panorama, and a more traditional dark bar set against a uniform bright panorama, although the textured bar had a more distinguishable bimodal distribution (Figure 1E; see Methods). Flies maintained an effectively stationary heading between saccades (Figure 1C,F) with the bar being fixated in the periphery (Figure 1E). Occasionally the bar would cross the visual midline of the animal, which the vast majority of time occurred when the fly initially detected the bar (Figure S1A).

Upon the bar entering the field of view, flies frequently generate an initial saccade oriented towards the bar, but occasionally will either not react or generate a saccade oriented away from the bar (Figure S1A,B). Here, we defined a successful bout of visual fixation as a continuous, syn-directional tracking effort through at least one half revolution (180°) around the arena (see Materials and Methods). Henceforth, we refer to this class of saccades as “bar-fixation saccades” on the basis of their distinct dynamics, trigger, frequency, and precision by comparison to spontaneous saccades. To our knowledge, bar-fixation saccades are previously undescribed in flies. Bar-fixation saccades in the magnetic tether were characterized by rapid changes in body orientation, generated by an initial, large angular acceleration, and followed by a small angular deceleration (Figure S1D–F).

Bar-fixation saccades differ from spontaneous saccades

We tested the hypothesis that body saccades are all-or-none events that are not tuned to motion dynamics of the bar stimulus. During visual fixation, with all bar speeds pooled, we measured a mean saccade duration of 77 ± 32 ms (median=69 ms), mean amplitude of $33 \pm 18^\circ$ (median = 28°), and a mean peak angular velocity of 567 ± 270 deg s⁻¹ (median = 509 deg s⁻¹). Saccade amplitude and duration were correlated (*t*-test for slope, $P < 0.001$; linear regression, $R^2 = 0.31$). Similarly, saccade amplitude and peak angular velocity were weakly correlated (*t*-test for slope, $P < 0.001$; linear regression, $R^2 = 0.17$), which is consistent with previous studies using a magnetic tether [10, 12](Figure S1C). We next presented flies with a stationary, randomly-patterned visual landscape. We detected and analyzed 6,852 spontaneous saccades ($n = 27$ animals; median number of saccades per trial = 9). Overall, spontaneous saccades were shorter, faster, and larger in amplitude than bar-fixation saccades (Figure 1G). Here we refer to “spontaneous saccades” as saccades that are not tied to any obvious external stimulus. For these saccades, we measured a mean saccade duration of 101 ± 53 ms (median = 83 ms), a mean amplitude of $64 \pm 34^\circ$ (median = 56°), and a mean peak angular velocity of 976 ± 457 deg s⁻¹ (median = 929 deg s⁻¹). The dynamics of spontaneous saccades were statistically different from saccades during a visual fixation task (*t*-test, $p < 0.001$ for saccade duration, amplitude, and peak angular velocity) (Figure 1G; Figure S1C). Bar-fixation saccades occurred at a rate well above the rate of spontaneous saccades (saccade rate in the presence of 30° width visual bar: median = 1.3 saccades s⁻¹; spontaneous saccade rate: median = 0.4 saccades s⁻¹, see section below). We compared the variation in amplitude, duration and peak angular velocity between bar-fixation and spontaneous saccades and found that bar-fixation saccades have much lower variation in these parameters, suggesting precise tuning to the visual stimulus (two-sample *F*-test for equal variances, $p < 0.001$ for amplitude, duration and angular velocity). On the basis of their dynamics, link to external stimulus, frequency and precision, we conclude that bar-fixation saccades are in a class different from spontaneous saccades.

Visual fixation saccades are tuned to bar motion dynamics

We discovered that body saccade dynamics are tuned to the bar velocity (Figure 1H). Bar velocity had a subtle but significant effect on saccade duration, amplitude, and peak angular velocity (ANOVA, $P < 0.001$ for all, $DF = 2$). When including the possible effects of individuals and stimulus direction, the statistical outcome did not change (mixed effect model, $P < 0.001$ for all). These results demonstrate that the dynamics of bar-fixation saccades are visually tuned to the dynamics of the bar stimulus.

A body saccade is initiated by a torque command, damped by aerodynamic forces and flapping counter-torque, and arrested by an active counter-torque [21, 30]. As expected, saccades executed in our flight arena were characterized by an initial torque followed by a counter torque (Figure 1I; Figure S1D–F). Since visual motion has very little effect during a saccade [17], any tuning should be planned prior to saccade execution. We tested the hypothesis that flies tune the initial torque to control saccade duration and amplitude. Initial peak torques were tuned to the bar speed (ANOVA, $P < 0.001$, $DF = 2$; Figure 1J; Figure S1G) and peak (minimum) counter- torques scaled with bar speed (ANOVA, $P < 0.001$, $DF = 2$; Figure 1J). In addition, further supporting the hypothesis that bar-fixation saccades are

tuned and are a different class of saccades, we found that the peak torques of these saccades were statistically smaller than those of spontaneous saccades (t -test, $p < 0.001$; fixation: $1.17 \times 10^{-8} \pm 5.78 \times 10^{-9}$ Nm, median = 1.04×10^{-8} Nm; spontaneous: $2.46 \times 10^{-8} \pm 3.07 \times 10^{-8}$ Nm, median = 1.84×10^{-8} Nm). Similarly, peak torques of bar-fixation saccades were statistically smaller than those of wide-field-motion-triggered optomotor saccades (t -test, $p < 0.001$; wide-field: $3.10 \times 10^{-8} \pm 4.05 \times 10^{-8}$ Nm, median = 2.11×10^{-8} Nm, see below for more on wide-field-motion-triggered saccades).

Fixation saccades are triggered by time integral of bar position error

Next, we tested the hypothesis that bar-fixation saccades are triggered by a threshold in the absolute retinal position error of the bar. Based on prior observations in rigidly-tethered flies that demonstrated a spatial ‘hotspot’ for triggering torque spikes [5, 8], we hypothesized that bar-fixation saccades in the magnetic tether might be triggered within a similar spatial domain. We measured the position error from the visual midline to the center of the bar prior to the execution of a saccade (bar width = 30°). During bouts of tracking a moving bar, pre-saccade retinal position error angles between the flies’ heading and the bar position were roughly 45° (Figure 2A), irrespective of the type of bar stimulus used (Figure S2A). Retinal position error angles and amplitude were weakly correlated (t -test for slope, $P < 0.001$; linear regression, $R^2 = 0.13$; Figure 2A) whereas pre- and post-saccade position error angles were strongly correlated (t -test for slope, $P < 0.001$; linear regression, $R^2 = 0.89$; Figure S2B). The magnitude of the pre-saccade retinal position error was subtly dependent on the speed of the bar (mixed-effect model, $P < 0.001$, $DF = 2$; Figure 2B,C). Furthermore, the inter-saccade intervals (ISI) scaled inversely with the speed of the bar (mixed effect model, $P < 0.001$; Figure 2D; Figure S2C).

The increase in retinal position error angle with increasing bar speed challenges the hypothesis that a threshold in retinal position error alone triggers a saccade. The decrease in ISIs for faster moving bars suggests that flies may instead integrate the retinal position error between their heading and the bar position to generate a saccade. Specifically, here we posit an explicit position controller that integrates bar position error over time. To test this hypothesis, we computed the temporal integral of bar position error angle between the end of each saccade and the start of the next saccade during bouts of bar fixation (Figure 2B showing baseline-subtracted error). The integrated retinal position error changed little as the speed increased (median integrated position error $\approx 2^\circ$ s, mixed-effect model, $P=0.261$, $DF = 2$; Figure 2E, Figure S2D). If flies do indeed compute the integrated retinal position error to trigger bar-fixation saccades, the origin of the variability in the proposed trigger is perplexing. In the mixed-effect model, individual animals had a marginally significant effect on the integrated retinal position error (mixed effect model, $P = 0.0431$), therefore individual animals contribute to some of the variability in the trigger. A challenge in identifying the source of the variability in the trigger is that it could arise from both external experimental influences and internal stochastic processes (see Discussion). Notwithstanding the presence of variability, our findings favor a mechanism whereby flies implement temporal integration of retinal position error within a narrow spatial field (Figure 2A) and that integrated retinal position error beyond a threshold generates a tuned fixation saccade.

We noticed that the measured integrated retinal position error magnitude does not equal the expected integrated retinal position error if one calculates the temporal integral directly from the error angle with respect to the visual midline and corresponding ISI (Figure 2C–D). In other words, a pre-saccade retinal position error of 40° (Figure 2C first column) over a time interval of 400 ms (Figure 2D first column) would predict an integrated retinal position error equal to 8°sec , rather than 2°sec we measured (Fig. 2E first column) (area under curve = $40^\circ \times 0.400\text{sec} / 2 = 8^\circ\text{sec}$). One possible explanation is that after a saccade, flies never end a saccade with the bar fixated on visual midline; indeed, flies were always offset and thereby perpetually lagged behind the bar (Figure 1B, D; Movie S1). Thus, during bar-fixation bouts, the position of the bar that triggers a saccade does not integrate from the fly's midline to the saccade-triggering angle, but rather through a smaller region of space offset from the visual midline. Based on the measured ISI range of $\sim 250\text{--}450$ ms and median integrated retinal position error of 2°s (Figure 2D), we predicted the region of space for integration to be approximately $9\text{--}16^\circ$. To confirm this, we measured the offset between the bar and the fly heading immediately after a saccade. The end-of-saccade, fly-to-bar offset was speed invariant, with a median of 26° (ANOVA, $P = 0.312$, $DF = 2$; mean \pm STD: $26^\circ \pm 14^\circ$; Figure S2E), which is consistent with the approximately linear scaling of saccade amplitude with bar speed (Figure 1H). This offset confirms our prediction that flies temporally integrated bar position through a narrow region of space following a saccade, and thereby provides some consistency in the reported magnitude of the integrated error (Figure 2E).

Optomotor saccades are triggered by integrated error and dynamically tuned to background speed

We demonstrated that bar fixation uses saccades tuned to visual motion and that bar motion itself generates little smooth movement between saccades (Figure 1C), but, in contrast, motion of the visual panorama should generate primarily smooth movement and only occasional saccades [26]. To determine if saccades generated by panoramic wide-field motion are triggered and tuned similarly, we presented flies a rotating visual landscape with no bar (Movie S2). Under these conditions, yaw-based gaze stabilization is enabled by a putative velocity controller whereby flies smoothly track the rotating landscape to minimize retinal slip but generate occasional body saccades (Figure 3A,B). As expected, flies operated at high gain to minimize retinal slip (Figure 3C–E). Overall, bouts of smooth movement lasted for an average period of 1.5 s before triggering a saccade in the same direction as the stimulus. We identified 2,232 syn-directional saccades across 10 animals (451 trials). These saccades had mean amplitude of 118° , mean duration of 140 ms and mean angular velocity of 856°s^{-1} , with dynamics similar to free flight saccades triggered by rotation of the full visual panorama [26]. Overall, visual rotation triggered more saccades than during the presentation of a static visual landscape, and this relationship was marginally speed dependent (Kruskal-Wallis test with grouped speeds, $P = 0.01$) (Figure S3A), suggesting that saccades were primarily visually guided but that some spontaneous saccades could be present. Overall, saccades were tuned to motion speed (ANOVA, $p < 0.001$ for amplitude, duration and peak angular velocity, $DF = 2$) (Figure 3F; Figure S3B,C). Saccades were triggered at heading angles spanning the entire arena, indicating that the arena provided approximately uniform yaw-based rotational stimuli, and that there was negligible mechanical bias in the magnetic tether (Figure S3E). Because there was precise tuning of

saccade dynamics according to motion dynamics, these results provide assurance that optomotor saccades are visually triggered rather than spontaneous in nature.

During rotation of the panorama, flies occasionally generated smaller, anti-directional saccades (Movie S3; 30% of all saccades; Figure S3C, F). Anti-directional saccades were less tuned to motion dynamics than syn-directional saccades (Figure S3G), and, interestingly, resembled the dynamics of bar-fixation saccades (Figure 1H). These anti-directional saccades occurred most frequently at low speeds where flies operated at the lowest gain (Figure 3E). These saccades were less prevalent than syn-directional optomotor saccades, so we cannot infer their functional role with confidence, but they may be analogous to optokinetic nystagmus whereby a drifting grating generates reflexive, anti-directional eye saccades.

Because optomotor saccades are visually guided, we hypothesized that they were triggered by a random process predicting the ISIs to be uniformly distributed across a range in time above the saccade refractory period of ~200 ms (see Results below for approximation of saccade refractory period). When measuring the distribution of ISIs with all speeds pooled, ISIs were not equally distributed but instead were biased asymmetrically toward smaller intervals (Figure S3H). Therefore, we rejected the hypothesis that optomotor saccades are generated by a random process with uniform distribution. Saccades were tuned to motion velocity and therefore we hypothesized that the same putative velocity controller that minimizes retinal slip generates occasional body saccades. We define angular velocity explicitly as the state variable of the control system to be consistent with prior literature and the established principle that motion detectors—which presumably drive the optomotor response—detect retinal slip [31]. To test the hypothesis that flies compute the integrated velocity error, we computed the integrated retinal slip error over time (units of degrees) driven by smooth movement between saccades (Movie S2). This analysis revealed that the pre-saccade integrated velocity error is speed invariant (Figure 3G; median error = 6°, ANOVA, $P = 0.201$, $DF = 2$), supporting the hypothesis that flies implement spatio-temporal integration to trigger optomotor saccades (Figure 3G).

Varying bar width highlights parallel saccade controllers

During bar fixation, flies generated little smooth movement between saccades (Figure 1C) whereas during rotation of the background, flies generated bouts of gaze-stabilizing smooth movement (Figure 3). What constitutes a ‘bar’ by comparison to a ‘background’? In particular, as the bar width increases, how is smooth and saccadic movement influenced? To answer this question, we parametrized bar width and revolved the bar in both clockwise and counterclockwise directions at an intermediate speed of 75°s^{-1} . Increasing the bar width concomitantly increased yaw-based smooth movement, whereas saccades were optimally triggered with bars spanning approximately 30–120° in width (Figure 4A).

The mean integrated retinal position error was speed invariant but saccade dynamics were speed dependent (Figure 1, 2), so we reasoned that saccade tuning may arise from the total integrated optic flow within a bar, which would scale with bar span. We therefore tested the prediction that wider bars moving at the same speed would generate larger saccade amplitudes, shorter duration, and larger angular velocities. We presented flies with bars

spanning 60, 90 and 120° in width moving at an intermediate velocity of $\pm 75^\circ\text{s}^{-1}$. These widths generated the highest rate of saccades and engaged some smooth movement (Figure 4A). Bar width had no effect on saccade dynamics (Figure 4B; ANOVA, duration: $P = 0.239$, amplitude: $P = 0.235$, peak angular velocity: $P = 0.550$, $DF = 2$; $n = 10$ animals, 2,575 saccades), thereby rejecting our initial hypothesis. A non-parametric Kruskal-Wallis test did not change the statistical outcome. Further, the pre-saccade integrated error was not sensitive to bar width (Figure 4C; ANOVA, integrated error, $P = 0.956$, $DF = 2$) and pre-saccade absolute error—measured from visual midline to the center of the bar—and ISIs varied little (Figure S4A–D; ANOVA, $P = 0.287$ & 0.193 , respectively, $DF = 2$). The absolute pre-saccade error was considerably larger than the pre-saccade error generated by narrower bars (Figure S4A,B), but the actual bar angle swept was consistent when considering the post-saccade error (Figure S4E). The post-saccade error varied little with bar width (Figure S4E) and the torque also varied little (Figure S4F). The finding that different bar widths generate the same saccade dynamics provides interesting insights into the mechanism of saccade tuning. The fact that saccade dynamics are bar speed dependent but not bar span dependent suggests that the saccade tuning mechanism does not integrate over the entire span of a bar, i.e. from leading to trailing edge. Instead, we propose that the spatial field for bar motion integration is finite (Figure 2A), activated by the bar leading edge, consistent with prior findings showing that a revolving ‘curtain’ elicits steering responses similar to those generated by a discrete bar [32].

When analyzing the tuning of saccades across the full range of bar width tested, we found that saccade amplitude is similar until about 120–150° (Figure 4D). Beyond this range, saccades begin to take on the character of optomotor saccades (Figure 3F). These results suggest that the fixation saccade control system operates within a range below 120°, which is consistent with the finding that the spatial action field for bar motion integration is small (Figure 2A). Interestingly, above 120°, saccades begin to be tuned to the overall optic flow rather than the bar speed, suggesting that another controller, one that is driven by a large region of the visual field, integrates the total optic flow within the bar. This result would be expected for a wide-field motion detector [33] and also for aspects of bar motion tracking that have been shown to depend upon the magnitude and direction of motion within the bar itself [34].

Flies rely on body saccades to fixate a bar on a counter-rotating background, but track the background smoothly between saccades

Next, to probe simultaneous bar fixation and optomotor tracking and thereby reveal the dynamics of the putative parallel controllers, we presented flies with a bar moving at constant speed superimposed on a counter-rotating ground of varying speed (Figure 5A; Movie S3). We tested three different ground speeds for the same bar speed (113°s^{-1}), which we had previously determined to generate robust, sustained bouts of bar fixation. From $N = 6,989$ saccades ($n = 10$ animals), we detected 1,361 bar-fixation saccades where flies continuously tracked the bar at least 180° around the arena. During inter-saccade intervals of bar fixation bouts, flies robustly tracked the ground in the direction opposite to bar motion (Figure 5B–D). Following the termination of a bar-fixation saccade, flies reacted to panoramic wide-field motion by reengaging the smooth movement in as little as 25 ms

(median latency) (Figure 5B), which is consistent with the minimum latency of steering responses to impulsive image displacements [34].

Overall, ground velocity had a marginally significant effect on saccade amplitude, duration, and peak angular velocity (ANOVA, amplitude: $P = 0.182$; duration: $P = 0.032$; peak angular velocity: $P = 0.011$, $DF = 2$)(Figure 5E). The average magnitude of the peak torque and counter torque scaled with the ground speed (ANOVA, $p < 0.001$ for both, $DF = 2$) (Figure 5F, G; Figure S5A). During bar fixation bouts, the ISIs were effectively constant for different background speeds (ANOVA, $P = 0.656$, $DF = 2$) and the triggering error angle scaled marginally with bar speed (ANOVA, $P = 0.017$; $DF = 2$)(Figure 5H; Figure S5B). The post-saccade error angle scaled with changing ground speed (Figure S5C) suggesting that flies end a saccade at the same heading relative to the bar. We subtracted the pre- from the post-saccade error angle and indeed found that the swept error angle actually varied little with ground speed (ANOVA, $P = 0.426$, $DF = 2$). We confirmed that the integrated error did not change across different ground speeds (mixed effect model, $p=0.897$)(Figure 5H), further supporting the hypothesis that spatio-temporal integration underlies saccade control. The integrated error threshold (Figure 5H) was smaller in the presence of a rotating ground compared to the case of bar alone (Figure 2E). While it is not immediately clear why the thresholds differ, we posit that the bar-ground stimulus, because it engages robust smooth movement between saccades, effectively shortens the time integration window because the fly is rotating away from the bar. This assumes that the spatial receptive field underlying integrated bar error computation is finite, which is supported by our data (Figure 2A; Figure S5B).

We had initially predicted that saccade dynamics would scale with ground speed because flies would experience different relative bar velocities during periods of inter-saccadic ground optomotor tracking at different ground speeds. While we found some evidence for this, it is not very compelling. One possible interpretation is that the fly's inertia has more of an effect under these stimulus conditions, which may explain why the post-saccade error angle scales with bar speed despite the bar speed being constant. Another possibility is that we pushed the neuromechanical system near its operating limit, which is suggested by the fact that ISIs remained constant across bar speed (Figure 5H). It is likely that flies have a refractory period which places an upper limit on saccade rate and therefore lower limit on ISIs. We found that ISIs plateau, suggesting a ~ 200 ms refractory period.

Hybrid integrate-and-fire computations model saccade control

To determine whether a simple mechanism could simultaneously capture the speed-invariant saccade trigger and the tuning of control torque according to bar or wide-field speed, we constructed a reduced-order, single mechanical degree-of-freedom model of the visual fixation task. Based on our behavioral results, a parsimonious model suggests parallel position and velocity controllers (Figure 6A). We determined that torque τ and saccade amplitude θ scale linearly in the behavior (Figure 1 H,J) and we therefore modeled the transform from τ to θ as a transfer function with simple linear scaling (Figure 6B). Our model assumed that during saccades flies operate in open-loop with respect to vision, which is supported by previous studies [17, 35]. Because saccades are discrete, i.e. non-continuous

unlike smooth movement, we modeled the fly as a hybrid dynamical system that exhibits both continuous and discrete dynamic behavior. We modeled the trigger as an integrate-and-fire mechanism linked to a two-state switch and simulated the position-based control system computationally (Matlab, Mathworks, Inc.)(Figure S6). The operation of the velocity-based controller would be similar in principle, with tuning of saccades from a signal proportional to rotational speed of the panorama (Figure 6A, dotted line). When the integrator reached a pre-determined constant threshold (C , Figure S6), it fired a control signal to trigger a change in switch position, allowing the error signal to flow for a short time interval to generate a scaled torque pulse command.

We modeled the open-loop bar position as a position ramp with different slopes (speeds), as generated in our experiment. The bar position was reset to the initial condition at every firing event, thus resetting the virtual position of the fly relative to the bar to initial conditions. One important point is that we model the mean integrated error but not the variability in the biological saccade trigger (Figure 2E) because at present it is unclear whether this stochasticity is due to internal biological processes or other external influences. This simple model was sufficient to capture our finding that flies visually tune saccades by (1) a constant-threshold saccade trigger mechanism and (2) tuning of torque commands that depends on bar speed (Figure 6C). All together, these results suggest that simple behavioral algorithms can account for the control of fixation saccades in *Drosophila*.

DISCUSSION

We discovered that flies that were free to steer on a magnetic pivot finely tuned the dynamics of body saccades both to fixate moving objects and compensate for slip of the panoramic flow field. Saccades were tuned to visual information, regulated by fine adjustments of the torque generated by the wings and were triggered when the temporal integral of either retinal angle error signal (for object) or panoramic slip velocity (for ground) reached a threshold that seems to be stochastic. In addition, we demonstrated a previously unknown switch between fixation saccades and smooth optomotor movement. We presented a novel reduced-order, hybrid control model that simulated both saccade tuning and triggering dynamics for both bar fixation and optomotor responses.

Saccade tuning

Fixation behavior has been characterized in a number of different species of flies while rigidly tethered [24] and freely flying [2, 4, 9, 36]. It has been proposed that a control system using both smooth movement and saccades may be near-optimal for visual fixation in both invertebrates and humans [3]. To our surprise, we observed that flies relied on saccades to fixate a salient visual object moving across a fixed visual landscape (Figure 1B) as there was little smooth yaw movement between saccades (Figure 1C). When moving a bar superimposed on a counter-rotating ground, however, we found that flies generate saccades to track the bar but also track the ground smoothly between saccades, switching between these two motor control strategies in as little as 25 ms (Figure 5A,B). Finally, by comparing the dynamics of bar-fixation saccades to those of spontaneous saccades, we determined that

bar-fixation saccades may fall into a different class as evidenced by their narrow distributions in amplitude, duration and peak angular velocity (Figure 1G).

Our results also provide evidence for precise visual tuning of saccades during bar fixation. By studying flight control in magnetically-tethered flies that were free to rotate in yaw, we were able to impose precise visual perturbations and record subtle changes in yaw dynamics. Consistent with our results (Figure 2A), previous studies showed that the amplitude of torque spikes, the behavioral analogue to saccades in rigidly-tethered flies, is proportional to the azimuthal position of a bar [8]. Similarly, studies in free flight showed that prior to landing on a post, *Drosophila* saccades scale with the angle of the post relative to the fly [9]. Therefore, it is probable that the rotating bar in our flight simulator triggers fixation saccades that are analogous to those generated in free flight during landing approach. Our results are also consistent with previous findings that the angular size of a saccade is controlled by adjusting the magnitude of the initial torque and subsequent counter-torque (Figure 1J) [21].

Saccade trigger

Our results reject the hypothesis that flies trigger fixation saccades according to absolute retinal position error. Instead, we found that both the absolute retinal position error and inter-saccade interval scale with the bar speed (Figure 2C,D). During bouts of bar fixation, the temporally integrated position error remained constant across different bar speeds (Figure 2E). In free-flight, flies generate targeted saccades that are triggered over a range of retinal sizes ($\sim 30\text{--}60^\circ$) consistent with the range we observed here [9]. Similarly, hoverflies chasing conspecifics generate saccades when the tracking error angle reaches approximately 50° [2]. Finally, the relative bar position error that elicits saccades in freely rotating flies is consistent with previous studies in rigidly-tethered flies revealing that torque spikes occur most frequently when a figure is located in the peripheral field of view, offset by about $\pm 60^\circ$ from flies' visual midline [8]. Each of these studies reasonably implicate the absolute retinal position for triggering saccades, but none parameterized the speed of the pursuit object, which would have been required to differentiate retinal position error from integrated retinal position error. Whereas the integrated retinal position error measurements are rather variable, the mean converges at roughly 2 degree seconds across a diverse set of experimental conditions (Figure 2E, 4C, 5H). An interesting avenue for future research will be to determine the source of variability in the trigger and tuning of saccades. We present deterministic models that simulate the mean of distributions, but we do not attempt to model the variability about the mean because its source is unclear and arises at least in part from individual animal variation. An interesting question is whether the saccade trigger is inherently stochastic. Finally, our quantification and modeling of the behavior does not preclude more complicated alternative control strategies. For instance, flies may tune saccades by computing additional terms, e.g. derivatives of object retinal position error, but teasing this out will require a more elaborate set of perturbations.

The notion that, as with the fixation of a vertical object, wide-field panoramic motion also triggers saccades at a set threshold of integrated error suggests that motion integration generalizes across two parallel control systems. We observed that the smooth tracking

component of the optomotor response would lag behind the stimulus and therefore flies could not maintain zero error; doing so would likely require prohibitively high closed-loop feedback gain that may in turn render the fly unstable to small perturbations [37]. We demonstrate that the putative input control signal for smooth optomotor movement—the integrated motion error—is bounded by smooth tracking and saccades as the integrated error accumulates. The error is bounded at around 6° (Figure 3G). To our knowledge, the time scale and magnitude of error accumulation during closed-loop optomotor tracking in *Drosophila* was not known at the level of precision that we have provided here. Thus we describe a previously unknown functional role for the switch between smooth movement and optomotor saccades, which prevents the integrated error signal to grow without bounds.

Saccades have been proposed to circumvent instabilities in the control system [3]. A study in larger flies posited that a single sensorimotor system may be responsible for generating smooth movement and fixation saccades [27]. Our results support the hypothesis that a velocity controller can generate both smooth movement and optomotor saccades, but that object fixation saccades are generated by another, parallel control system, thereby supporting the hypothesis by Land [3]. The hybrid control system we propose would contain a wide-field motion integrating component and a saccade generating component of as yet unknown origin (Figure 6A).

Switch between smooth and saccadic movement

The result that flies primarily rely on saccades for bar fixation on a fixed visual landscape rather than a combination of smooth movement and saccades was not expected (Fig. 1A–D). Primate eyes, in contrast, rely on smooth movement and saccadic eye movement to pursue visual bars [1]. When rotating a narrow bar against a counter-rotating visual landscape, flies switch between smooth movement and saccades (Figure 5). Specifically, flies rely on saccades to track the bar but rapidly engage the smooth optomotor reflex between saccades with a delay as small as 25 ms, consistent with other methods of measurement [7]. During inter-saccadic smooth movement, flies are still capable of perceiving and fixating a visual bar, the corollary of which is that bar tracking is little perturbed by movement of the visual panorama [29]. Robustly tracking the ground in closed-loop would reduce ground motion on the retina and thereby enhance the visual salience of a moving bar. Systematically increasing bar width revealed that saccades are optimally generated within the range of approximately $30\text{--}120^\circ$, whereas the smooth movement system engages more robustly with larger bar widths (Figure 4A). This finding is broadly consistent with recent experiments on rigidly tethered flies in which the balance between bar fixation and optomotor stabilization varies continuously over bar width [29].

Why do flies predominantly use saccadic fixation instead of a combination of smooth and saccadic pursuit? Our results suggest that the contrasting visual panorama engages the smooth optomotor system under closed-loop feedback conditions, at high gain. Therefore, any smooth object pursuit would inescapably generate a counter-acting turn by engaging the corrective, wide-field-motion-sensitive optomotor reflex, and thereby nullifying any volitional movements. The counter-acting turns could be potentially disengaged by making use of an efference copy to suppress reafferent visual information [35, 38], but this seems

not to be the case for object fixation. Another possibility is that from a control standpoint, there is an inherent advantage in fixating bars via saccades. It has been demonstrated that smooth movement systems with continuous visual feedback are inherently unstable, particularly when operating with realistic delays and at higher frequencies [3]. Land suggested that one way animals overcome the inherent instability of smooth movement is to generate rapid saccades during which visual feedback is suspended and self-generated eye motion suppressed. Of course, this visual tracking strategy would tradeoff stability for continuous visual feedback as the bar motion may be imperceptible during a saccade [17, 35].

Comparison of bar fixation in rigidly- and magnetically-tethered flies

In response to the presentation of a rotating bar under open-loop conditions, rigidly-tethered flies will adjust their wingbeat kinematics in an attempt to track the bar. Previous studies showed that changes in wingbeat amplitude appear to be smooth and periodic as the bar oscillates periodically across the visual midline, suggesting the engagement of a smooth optomotor response [6]. These observations in rigidly-tethered flies seem at odds with our current finding demonstrating saccadic fixation of bars, with little or no smooth movement near visual midline. This apparent discrepancy can be resolved in part if we consider that analyses of rigidly tethered flies typically average the time course of the wing beat amplitude (WBA) signals across trials and individuals, therefore effectively low-pass filtering WBA signals. With averaging, the presence of higher-frequency torque spikes — the behavioral analog to body saccades [10]—become difficult to distinguish. When one analyzes the WBA signal from a single trial from an individual fly, the signal contains step-like, torque spikes (e.g.[8]). The same phenomenon occurs in the magnetic tether apparatus, wherein periodic bar oscillation generates, on average, smooth variation in heading angle [39]. Therefore, averaging of WBA signals— while useful to detect effects across trials and individuals—must be interpreted with caution with regards to the motor strategy used by flies for visual fixation.

WBA averaging cannot, however, explain the finding that in our experimental situation flies do not fixate the bar on visual midline (Figure 1E) the way they do when rigidly tethered [11, 24, 29, 40]. Not only is the fixation histogram bimodal for magnetically tethered flies, they seem to ignore motion cues generated by the bar as it sweeps across midline (Figure 1F). This finding contradicts prior studies that demonstrate unequivocally that rigidly tethered flies modulate WBA robustly in response to either small-field motion contained within a bar centered on visual midline or a bar oscillated about visual midline [34], and fixate the bar on midline even when ground motion moves in the opposing direction [29, 40].

We cannot yet fully explain why a bar moving across visual midline fails to provoke a robust smooth optomotor fixation response in the magnetic tether apparatus, whereas it clearly does so for a rigidly fixed fly, which is what generates the classical unimodal fixation histogram [5]. We would point out, however, that magnetically tethered flies are under active, *naturalistic* closed-loop feedback conditions with respect to the visual panorama, i.e. steering results in dynamically naturalistic reafferent visual and mechanosensory feedback.

By contrast, rigidly fixed flies are under *virtual* closed-loop feedback conditions, i.e. changes in WBA are coupled to reafferent feedback through an imposed visual gain, without any mechanosensory reafference. Our working model is that the wide-field motion detection system is operating in open-loop in rigidly tethered flight, and is engaged by a revolving bar [40], resulting in directionally-selective smooth tracking responses that are strongest in the frontal field of view [8], thereby resulting in fixation. By contrast, during magnetically tethered flight, the optomotor system is always engaged in closed-loop by the full-size visual panorama [29], and so the bar is ‘ignored’ by the wide-field motion detection system and engages only the higher-order figure motion subsystem [8] that triggers saccades when the bar appears in the visual periphery and crosses the integrated error threshold.

Effect of constraining dynamics in magnetically-tethered flight

Studying flight in tethered preparations is desirable to systematically parametrize the analysis of behavior, yet raises the question of which components of the sensorimotor loop present during free flight are lost or altered by constraining the behavior. For instance, free flight combines rotational and translational motion cues but here only rotational cues were investigated. Despite these limitations, we observed saccade dynamics that were similar to those measured in free flight. For instance, saccade amplitudes ranged from about 30° for bar-fixation saccades, to 60° for spontaneous saccades, to well over 100° for optomotor saccades, which compare to free flight averaging about 90° [21]. Free-flight saccades are banked turns involving rotation about the yaw, pitch and roll axes [21, 22, 41], but the magnetic tether limits rotation to the yaw axis, which a recent study showed to be the slower phase during free flight saccades [21]. Also, tethered flies use a “clap and fling” stroke where the wings make contact at the peak of the upstroke [10, 42]. Under these conditions, flies generate a large pitch moment that may interfere with the production of yaw torques [43]. The duration of saccades measured here tended to be longer than those measured in free flight [21], which could be due to constrained haltere feedback, particularly as halteres are most sensitive to rotations along the pitch and roll axes [44]. Thus, our estimates of torque must be interpreted with appropriate caution. Yet, our measurements of angular acceleration demonstrate that saccades in the magnetic tether are inertial and arrested by a rapid, active deceleration of the body (Figure S1F) in a way similar to free flight saccades [30]. Notwithstanding these important caveats, our results would likely generalize to free flight conditions, particularly since initial torque production and turn angle both scale across all three axes of rotation [21].

Neural control hypotheses

We determined that a switched (hybrid), integrate-and-fire model is sufficient to explain saccade control during a visual object fixation task (Figure 6A). Specifically, our findings evoke a small-field-motion sensitive system for object fixation in which flies visually tune saccades using (1) integrated-object-error-based saccade trigger mechanism and (2) tuned torque commands that depend on absolute object error (Figure 6A). This model provides a plausible circuit that accounts for the control of bar-fixation saccades. Our findings suggest a parallel wide-field-motion controller that guides both optomotor tracking and optomotor saccades. As with the bar tracking controller, the wide-field-sensitive optomotor controller would generate a saccade when the integrator reaches a set threshold, albeit in velocity

rather than position, with tuning to background motion velocity. We posit that these two controllers always operate in parallel because 1) optomotor stabilization is essential for enhancing visual salience of objects (Figure 5A) and 2) optomotor tracking is engaged even when a very narrow bar is present in the periphery (Figure 4A). While we propose a deterministic model for the trigger of saccade, we note that the parameter for triggering saccades (integrated retinal position error) is quite variable (Figure 2E; Figure 3G). Although it is difficult to distinguish the source of this variability—it could arise from the magnetic tether restricting saccade dynamics, variation in preparations, individual animal variation, etc.—an interesting avenue for future research will be to determine whether trigger timing variability arises from endogenous stochastic processes in saccade control circuits.

One recent study has identified descending neurons whose activity correlates with spontaneous saccades [19]. At present it is unknown what neural center could provide the trigger for bar-fixation saccades. We posit that the object-tracking tracking system should 1) exhibit no directional selectivity (Figure S1A), 2) have narrow bilateral receptive fields offset by approximately $\pm 45^\circ$ (Figure 2A), 3) be sensitive to bar motion irrespective of wide-field motion (Figure 5), and 4) integrate position error (Figure 2E). Small-object sensitive neurons have recently been discovered in the lobula of *Drosophila* therefore the lobula may be a good candidate to implement tuning of visually-guided saccades during object fixation [45, 46]. In contrast, the wide-field system should respond weakly to bar motion (Figure 4A) and integrate wide-field motion velocity. An obvious potential system for wide-field integration is the directionally selective wide-field cells of the lobula plate, at least one of which has been shown to act as an integrator of horizontal motion [31].

STAR Methods

Contact for Reagent or Resource Sharing

Further information and requests of data, software, and reagents should be directed to and will be fulfilled by the Lead Contact, Mark Frye (frye@ucla.edu).

Experimental Model and Subject Details

A wild-type *Drosophila melanogaster* Meigen strain was maintained at 25°C under a 12 h: 12 h light:dark cycle with access to food and water *ad libitum*. All experiments were performed with 3- to 5-day-old female flies.

Methods Details

Animal preparation—We prepared the animals for each experiment according to a protocol that has been previously described [28]. Briefly, we cold-anesthetized the flies by cooling them on a Peltier stage maintained at approximately 4°C. We glued stainless steel minuten pins (100 μ m diameter, Fine Science Tools, Foster City, CA) onto the thorax by applying UV-activated glue (XUVG-1, Newall). The pin was placed on the thorax projecting forward at an angle of approximately 30°, which is similar to the body's angle of attack during free flight [22]. The pin's length was approximately 1 cm to minimize the moment arm about which the fly can generate cross-field torques in pitch and roll. The pins were less

than 1 percent of the fly's moment of inertia about the yaw axis. Flies were allowed at least one hour to recover before running experiments.

Flight arena—The magnetic-tether arena has been described elsewhere [10, 28]. Briefly, the display consists of an array of 96×16 light emitting diodes (LEDs, each subtending 3.75° on the eye) that wrap around the fly, subtending 360° horizontally and 60° vertically (Figure 1A). Flies were suspended between two magnets, allowing free rotation along the vertical (yaw) axis. We illuminated the fly from below with an array of eight 940 nm LEDs. We video-recorded the angular position of the fly within the arena at $160 \text{ frames s}^{-1}$ with an infrared-sensitive camera placed directly below the fly (A602f, Basler, Ahrendburg, Germany).

Experimental protocol—After suspending the fly within the magnetic field, we gave the flies several minutes to acclimate. We began each experiment by eliciting sustained rotation of the fly by rotating a visual panorama either clockwise or counterclockwise for 30 s at 120° s^{-1} . From these data, we estimated the fly's point of rotation by computing the cumulative sum of all frames and measuring its centroid. We elicited rotation by rotating a vertical pole of expansion and contraction that was separated by 180° . Previous studies have shown that flies actively avoid the pole of expansion [47]. This stimulus elicited a strong rotatory, yaw-based optomotor response. Flies that could not robustly track the pole of contraction throughout the arena were not used in experiments.

In a preliminary experiment, we determined that a motion-defined bar (textured moving bar superposing on a similarly textured static background) elicited ~50% more bar-fixation saccades than a dark bar on a uniform ground therefore we used the former stimulus to study saccade control (1,205 vs. 617 saccades, respectively; $n = 12$ animals, 112 trials, balanced design). From our subsequent experiment using the motion-defined bar, we detected a total of 2,968 bar-fixation saccades ($n = 10$ animals; median number of saccades per 30 s trial = 40). This number of fixation saccades represented 47% of the total saccades identified across all trials and individuals, suggesting that in our setup a large portion of body saccades are generated to robustly fixate the bar.

Visual stimulation—In the magnetic tether, we elicited visual bar fixation by rotating a motion-defined, 8-pixel-wide (30°) vertical bar on a randomly-generated background of 'on' and 'off' pixels. The stimuli were one dimensional in that they varied only in azimuth, were identical in elevation (i.e. all texture was oriented vertically and moved horizontally). The bar's initial position was generated from a pseudo-random sequence. To determine the dynamics of saccades elicited by rotation of a wide-field stimulus, we presented a randomly-textured panorama. We presented all stimuli at three different angular velocities. We randomized the order, direction, and speed of each stimulus to minimize habituation. We presented each stimulus for a period of 30 s, defining the duration of an individual trial. Between each trial, we presented a fixed visual landscape for 25 s for the fly to rest. To determine the performance of bar fixation on a counter-rotating ground, we moved the ground at three different velocities ($38, 75, 113^\circ \text{ s}^{-1}$) while the bar moved at a fixed speed 113° s^{-1} . We had previously determined that this bar speed elicits robust bar fixation on a fixed visual landscape. To determine the dynamics of spontaneous saccades, we displayed a

fixed visual landscape consisting of a random pattern of on and off pixels and recorded the fly's angular position for 30 s. Only flies that flew continuously for at least 10 trials were included in the analysis. If flies stopped flying during a trial, the trial was discarded. We ignored the first 5 s of a trial in order to avoid the inclusion of spontaneous saccades which could be generated when the stimulus first appears.

Quantification and Statistical Analysis

Saccade analysis—To identify saccades, we analyzed the angular position data using custom scripts (Matlab, Mathworks, Natick, MA, USA). Briefly, to calculate the orientation of the fly, we converted each frame to a binary image and modeled the shape of the fly as an ellipse. We manually defined the head orientation relative to the center of rotation in the first frame to set the initial conditions. We applied a low-pass, Butterworth filter with a cutoff frequency of 25 Hz to the position data and took the derivative of the filtered data to identify saccade events. To define a saccade-detection threshold, we estimated the standard deviation of the background noise of the velocity data for each trial. We defined the noise floor σ_n as

$$\sigma_n = \text{median} \left(\frac{|x|}{0.6745} \right) \quad (1)$$

where x is the filtered signal, which provides a robust estimate of the noise floor in the presence of spiking events [48]. We defined the threshold as four times the estimated noise floor. We then determined the peak of a velocity spike by computing the local maxima. We defined the period of a saccade as the time when fly's angular velocity was greater than one quarter of the peak amplitude, a method which has been adopted previously and that we found to work adequately [10]. We rejected saccades below 10° and above 180° in order to avoid the possible inclusion of tracking error into our dataset. To determine the delay between the termination of a saccade and the engagement of the optomotor reflex during the simultaneous presentation of a moving bar superimposed on a moving ground, we estimated the time between the termination of the saccade ($1/4$ of peak angular velocity) and the local maximum of the fly heading, corresponding to the transition to smooth movement (Figure 5B). This measurement provides a conservative estimate of the switching delay.

To estimate a fly's torque, we modeled the rigid body dynamics of the fly as

$$\tau = I\ddot{\theta} + C\dot{\theta} \quad (2)$$

where θ is the yaw angle, I is the moment of inertia, C is the linear rotational damping and τ is the wing-generated torque. We used values for I (1.0×10^{-12} Nm·s²) and C (5.2×10^{-12} Nm·s) that have been estimated for a magnetic-tether apparatus identical to ours [10, 49]; in the magnetic tether, the ratio of inertial (I) to viscous forces (C) yields a time constant of 0.2 s [10], which is significantly longer than the duration of a saccade. These constants take into consideration the effects of magnetic, gravitational, and aerodynamic forces as well as the offset from the point of rotation to the center of mass in estimating the moment of inertia [10].

To define bouts of bar fixation, we measured the correlation between the fly position and the bar position signals using a sliding, non-overlapping window (window width = 180°). We defined robust tracking when 95% of the variance was captured by linear regression analysis and the fly tracked continuous tracked bar for at least half a revolution around the arena (180°), corresponding to approximately five tracking saccades. The statistical outcome of our study did not change when including saccades where the fly tracked the bar continuously for either one quarter of a revolution (90°) or a full revolution (360°). Only saccades syn-directional to the bar were included in the final analysis. In few cases (2/181 trials), flies continuously anti-tracked the bar. We computed integrals using trapezoidal numerical integration. Head movement was very small compared to body movement, therefore we did not include head movement in our analysis of integrated retinal position error (mean \pm 1 STD = 1.1° \pm 1.9°; n = 5 flies, 40 trials).

Statistical Analysis—All statistical analysis was performed using Matlab (Mathworks, Natick, MA, USA) and JMP (SAS, Cary, NC, USA). For statistical analysis, we treated each saccade as an independent sample and evaluated the effect of individuals using mixed-effect models where individuals were modeled as random factors. Unless otherwise noted, data were plotted after taking the average for each individual across trials (e.g. box plots), thereby avoiding pseudoreplication. For box plots, the central line is the median, the bottom and top edges of the box are the 25th and 75th percentiles and the whiskers extend to the lowest and highest datum within 1.5×IQR (inter-quartile range) or approximately \pm 2.7×STD (standard deviation).

Supplementary Material

Refer to Web version on PubMed Central for supplementary material.

Acknowledgments

We thank undergraduates Allie Solomon and Farhaad Khan for laboratory assistance. This work was funded by the National Institutes of Health EY026031, the US Army Research Office W911NF-15-1-0558, and the National Science Foundation IOS-1455869.

References

1. Orban de Xivry J-J, Lefèvre P. Saccades and pursuit: two outcomes of a single sensorimotor process. *J. Physiol.* 2007; 584:11–23. [PubMed: 17690138]
2. Collett TS, Land MF. Visual control of flight behaviour in the hoverfly *Syrretta pipiens* L. *J. Comp. Physiol. A.* 1975; 99:1–66.
3. Land MF. Visual tracking and pursuit: Humans and arthropods compared. *J. Insect Physiol.* 1992; 38:939–951.
4. Maimon G, Straw AD, Dickinson MH. A simple vision-based algorithm for decision making in flying *Drosophila*. *Curr. Biol.* 2008; 18:464–70. [PubMed: 18342508]
5. Reichardt W, Poggio T. Visual control of orientation behaviour in the fly. Part I. A quantitative analysis. *Q. Rev. Biophys.* 1976; 9:311–75. 428–38. [PubMed: 790441]
6. Duistermars BJ, Reiser MB, Zhu Y, Frye MA. Dynamic properties of large-field and small-field optomotor flight responses in *Drosophila*. *J. Comp. Physiol. A.* 2007; 193:787–799.
7. Theobald JC, Ringach DL, Frye MA. Dynamics of optomotor responses in *Drosophila* to perturbations in optic flow. *J. Exp. Biol.* 2010; 213:1366–1375. [PubMed: 20348349]

8. Aptekar JW, Shoemaker PA, Frye MA. Figure tracking by flies is supported by parallel visual streams. *Curr. Biol.* 2012; 22:482–487. [PubMed: 22386313]
9. van Breugel F, Dickinson MH. The visual control of landing and obstacle avoidance in the fruit fly *Drosophila melanogaster*. *J. Exp. Biol.* 2012; 215:1783–1798. [PubMed: 22573757]
10. Bender JA, Dickinson MH. Visual stimulation of saccades in magnetically tethered *Drosophila*. *J. Exp. Biol.* 2006; 209:3170–82. [PubMed: 16888065]
11. Heisenberg M, Wolf R. On the fine structure of yaw torque in visual flight orientation of *Drosophila melanogaster*. *J. Comp. Physiol. A.* 1979; 130:113–130.
12. Mayer M, Vogtmann K, Bausenwein B, Wolf R, Heisenberg M. Flight control during “free yaw turns” in *Drosophila melanogaster*. *J. Comp. Physiol. A.* 1988; 163:389–399.
13. Briand KA, Strallow D, Hening W, Poizner H, Sereno AB. Control of voluntary and reflexive saccades in Parkinson’s disease. *Exp. Brain Res.* 1999; 129:38–48. [PubMed: 10550501]
14. Censi A, Straw AD, Sayaman RW, Murray RM, Dickinson MH. Discriminating External and Internal Causes for Heading Changes in Freely Flying *Drosophila*. *PLoS Comput. Biol.* 2013; 9
15. Tammero LF, Dickinson MH. The influence of visual landscape on the free flight behavior of the fruit fly *Drosophila melanogaster*. *J. Exp. Biol.* 2002; 205:327–343. [PubMed: 11854370]
16. Tammero LF, Dickinson MH. Collision-avoidance and landing responses are mediated by separate pathways in the fruit fly, *Drosophila melanogaster*. *J. Exp. Biol.* 2002; 205:2785–2798. [PubMed: 12177144]
17. Bender JA, Dickinson MH. A comparison of visual and haltere-mediated feedback in the control of body saccades in *Drosophila melanogaster*. *J. Exp. Biol.* 2006; 209:4597–606. [PubMed: 17114395]
18. Heisenberg M, Wolf R. Reafferent control of optomotor yaw torque in *Drosophila melanogaster*. *J. Comp. Physiol. A.* 1988; 163:373–388.
19. Schnell B, Ros IG, Dickinson MH. A Descending Neuron Correlated with the Rapid Steering Maneuvers of Flying *Drosophila*. *Curr. Biol.* 2017; 27:1200–1205. [PubMed: 28392112]
20. Martinez-Conde S, Otero-Millan J, Macknik SL. The impact of microsaccades on vision: towards a unified theory of saccadic function. *Nat. Rev. Neurosci.* 2013; 14:83–96. [PubMed: 23329159]
21. Muijres FT, Elzinga MJ, Iwasaki NA, Dickinson MH. Body saccades of *Drosophila* consist of stereotyped banked turns. *J. Exp. Biol.* 2015; 218:864–75. [PubMed: 25657212]
22. Fry SN, Sayaman R, Dickinson MH. The aerodynamics of free-flight maneuvers in *Drosophila*. *Science.* 2003; 300:495–8. [PubMed: 12702878]
23. Kern R, Boeddeker N, Dittmar L, Egelhaaf M. Blowfly flight characteristics are shaped by environmental features and controlled by optic flow information. *J. Exp. Biol.* 2012; 215:2501–2514. [PubMed: 22723490]
24. Gotz KG. Flight control in *Drosophila* by visual perception of motion. *Kybernetik.* 1968; 4:199–208. [PubMed: 5731498]
25. Geiger G, Nässel DR. Visual orientation behaviour of flies after selective laser beam ablation of interneurons. *Nature.* 1981; 293:398–9. [PubMed: 7278992]
26. Mronz M, Lehmann F-O. The free-flight response of *Drosophila* to motion of the visual environment. *J. Exp. Biol.* 2008; 211:2026–2045. [PubMed: 18552291]
27. Boeddeker N, Egelhaaf M. A single control system for smooth and saccade-like pursuit in blowflies. *J. Exp. Biol.* 2005; 208:1563–1572. [PubMed: 15802679]
28. Duistermars BJ, Frye M. A Magnetic Tether System to Investigate Visual and Olfactory Mediated Flight Control in *Drosophila*. *J. Vis. Exp.* 2008; 33:41–6.
29. Fox JL, Aptekar JW, Zolotova NM, Shoemaker PA, Frye MA. Figure-ground discrimination behavior in *Drosophila*. I. Spatial organization of wing-steering responses. *J. Exp. Biol.* 2014; 217:558–69. [PubMed: 24198267]
30. Cheng B, Fry SN, Huang Q, Deng X. Aerodynamic damping during rapid flight maneuvers in the fruit fly *Drosophila*. *J. Exp. Biol.* 2010; 213:602–12. [PubMed: 20118311]
31. Schnell B, Weir PT, Roth E, Fairhall AL, Dickinson MH. Cellular mechanisms for integral feedback in visually guided behavior. *Proc. Natl. Acad. Sci. U. S. A.* 2014; 111:5700–5. [PubMed: 24706794]

32. Aptekar JW, Keles MF, Lu PM, Zolotova NM, Frye MA. Neurons forming optic glomeruli compute figure-ground discriminations in *Drosophila*. *J. Neurosci.* 2015; 35:7587–99. [PubMed: 25972183]
33. Hassenstein B, Reichardt W. Systemtheoretische Analyse der Zeit-, Reihenfolgen- und Vorzeichenbewertung bei der Bewegungsperzeption des Rüsselkäfers *Chlorophanus*. *Zeitschrift für Naturforsch.* 1956; B 11
34. Theobald JC, Shoemaker PA, Ringach DL, Frye MA. Theta motion processing in fruit flies. *Front. Behav. Neurosci.* 2010; 4
35. Kim AJ, Fitzgerald JK, Maimon G. Cellular evidence for efference copy in *Drosophila* visuomotor processing. *Nat. Neurosci.* 2015; 18:1247–55. [PubMed: 26237362]
36. Boeddeker N, Kern R, Egelhaaf M. Chasing a dummy target: smooth pursuit and velocity control in male blowflies. *Proc. Biol. Sci.* 2003; 270:393–399. [PubMed: 12639319]
37. Aström, KJ., Murray, RM. *Feedback Systems: An Introduction for Scientists and Engineers.* Princeton University Press; 2010.
38. von Holst E, Mittelstaedt H. The principle of reafference: interactions between the central nervous system and the peripheral organs. *Naturwissenschaften.* 1950; 37:464–467.
39. Theobald JC, Duistermars BJ, Ringach DL, Frye MA. Flies see second-order motion. *Curr. Biol.* 2008; 18:R464–5. [PubMed: 18522814]
40. Fenk LM, Poehlmann A, Straw AD. Asymmetric processing of visual motion for simultaneous object and background responses. *Curr. Biol.* 2014; 24:2913–9. [PubMed: 25454785]
41. Schilstra, Hateren. Blowfly flight and optic flow. I. Thorax kinematics and flight dynamics. *J. Exp. Biol.* 1999; 202(Pt 11):1481–90. [PubMed: 10229694]
42. Weis-Fogh T. Quick estimates of flight fitness in hovering animals, including novel mechanisms for lift production. *J. Exp. Biol.* 1973; 59:169–230.
43. Fry SN. The aerodynamics of hovering flight in *Drosophila*. *J. Exp. Biol.* 2005; 208:2303–2318. [PubMed: 15939772]
44. Sherman A, Dickinson MH. A comparison of visual and haltere-mediated equilibrium reflexes in the fruit fly *Drosophila melanogaster*. *J. Exp. Biol.* 2003; 206:295–302. [PubMed: 12477899]
45. Kele MF, Frye MA. Object-Detecting Neurons in *Drosophila*. *Curr. Biol.* 2017; 27:680–687. [PubMed: 28190726]
46. Wu M, Nern A, Williamson WR, Morimoto MM, Reiser MB, Card GM, Rubin GM. Visual projection neurons in the *Drosophila* lobula link feature detection to distinct behavioral programs. *Elife.* 2016; 5
47. Tammero LF, Frye MA, Dickinson MH. Spatial organization of visuomotor reflexes in *Drosophila*. *J. Exp. Biol.* 2004; 207:113–122. [PubMed: 14638838]
48. Quiroga RQ, Nadasdy Z, Ben-Shaul Y. Unsupervised spike detection and sorting with wavelets and superparamagnetic clustering. *Neural Comput.* 2004; 16:1661–87. [PubMed: 15228749]
49. Bender, JA. *Elements of feed-forward and feedback control in Drosophila body saccades.* California Institute of Technology; 2007.

Highlights

- Under naturalistic conditions, object fixation is enabled by body saccades
- Saccade dynamics are finely tuned to object dynamics
- Saccades are triggered by the temporal integral of object position
- Object fixation and ground stabilization is enabled by parallel controllers

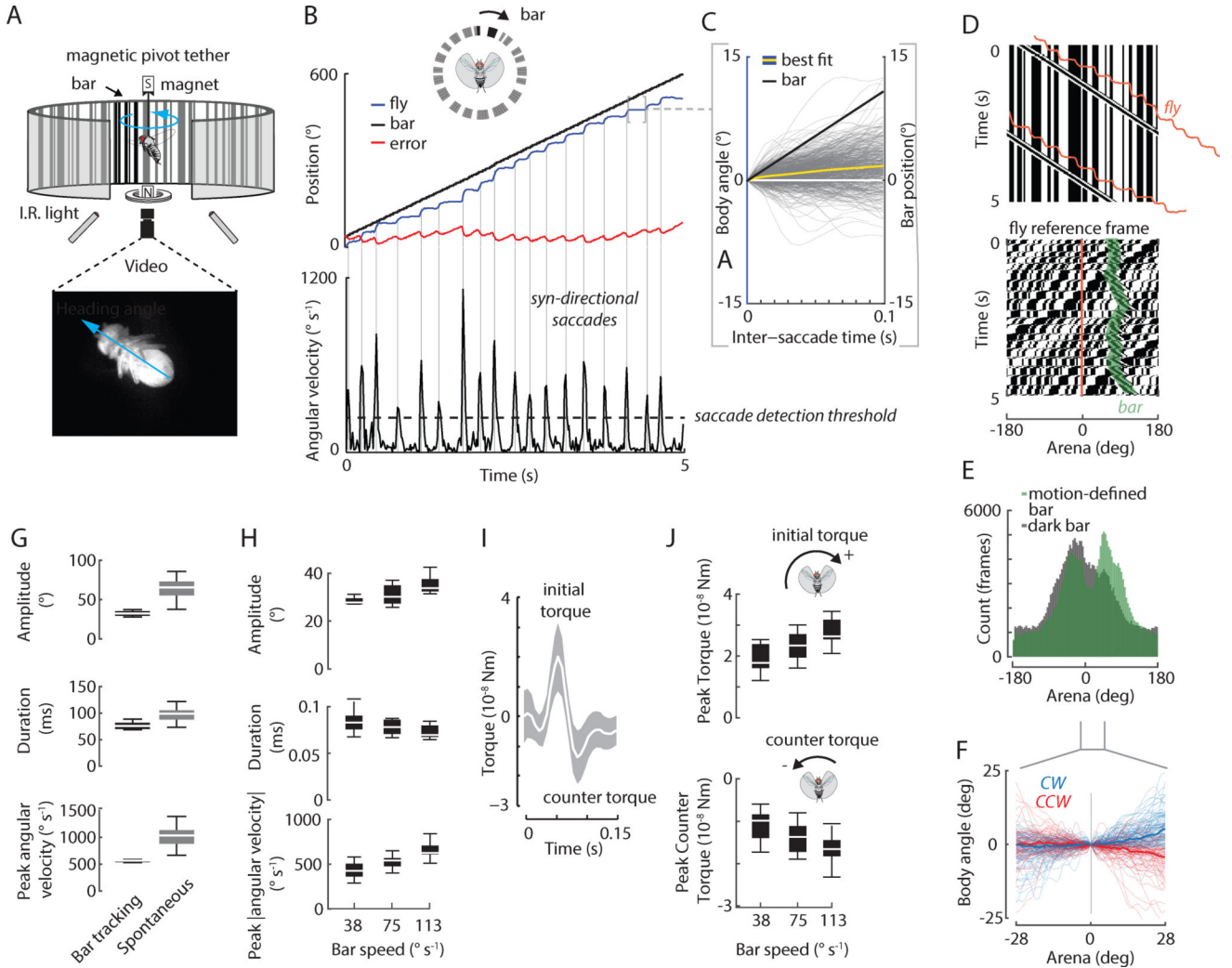


Figure 1. Flies generate bar-fixation saccades that are different than spontaneous saccades and dynamically tuned to bar motion

A) Arena to study visual fixation of bar with the fly free to rotate in yaw. The fly is suspended within a magnetic field and illuminated from below with infrared lights. A bar of random “on” and “off” pixel columns is superimposed over a similarly randomly-generated background. B) Top panel: fly heading (blue), relative bar position (black), and error angle (red) between the fly and the bar during bar fixation. Bottom panel: filtered velocity data. Horizontal dashed line: threshold for detecting saccades. Vertical lines: identified saccades. C) Body angle (blue) and bar reference angle (black) between saccades: during bar fixation. The yellow line is the best-fit line through the body angle data. D) Top: space-time graph of bout shown in B. Each pixel row represents the azimuthal distribution of “on” and “off” pixels displayed in the arena at a point in time. Slanted lines indicate clockwise bar rotation over time. Vertical lines indicate the stationary background over time. The fly trajectory is shown in orange. Bottom: space-time graph of bout shown in B, but in fly’s visual reference frame (orange). The bar is highlighted in green shading for visual comparison. E) Histogram of bar position in fly reference frame for motion-defined and traditional dark bar stimuli, indicated with cartoons. Bar rotation velocity is $\pm 75^\circ\text{s}^{-1}$. $n = 12$ animals with balanced

experimental design. 112 trials (56 motion-defined bar, 56 dark bar). We analyzed CW and CCW data together and show the distribution of signed bar position with respect to the fly visual midline. F) Trajectory of body angle for instances in which the motion-defined bar passed across visual midline between saccades for clockwise (CW) and counter-clockwise (CCW) bar rotation. Thin lines are from individual flight trajectories, thick lines are means. To emphasize the contribution of smooth movement, fly trajectories are plotted within a narrow spatial window where saccades are less frequently generated (see Figure 2A). G) Box plot of saccade amplitude, duration, and angular velocity for bar fixation (black) and spontaneous (grey) saccades. The dynamics of bar-fixation saccades were statistically different from spontaneous saccades. Bar-fixation saccades: 2,968 saccades from 10 animals. Spontaneous saccades: 4,137 saccades from 23 animals. H) Body saccade dynamics are tuned to the bar velocity. Bar velocity had a significant effect on saccade duration, amplitude, and peak angular velocity (ANOVA, $P < 0.001$ for all). I) Flies generate an initial torque followed by a counter torque. The white line shows the mean torque. Shaded areas are ± 1 STD. J) Initial peak torques are tuned to the bar speed ($p < 0.001$). Peak (minimum) counter-torques scale with bar speed ($p < 0.001$). Except for E), $n = 2,968$ saccades from 10 animals. See also Figure S1 and Movie S1.

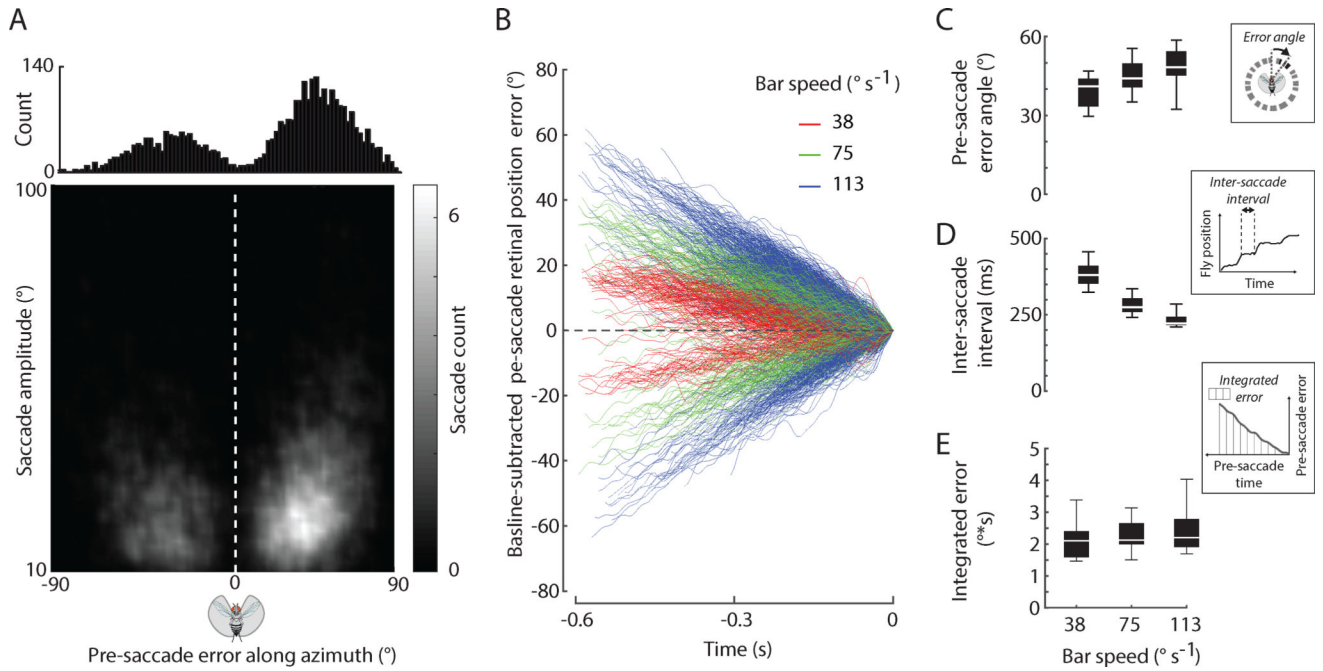


Figure 2. Bar-fixation saccades are triggered by a time integral of bar position error

A) The distribution centers of saccade-triggered error angles along the visual azimuth during bouts of visual fixation. Error angles between the flies' heading and the bar position were offset by approximately $\pm 45^\circ$. Shaded bar indicates the number of saccades. Error is computed between visual midline and bar center. Bar width = 30° . B) The error angle between the bar and fly's heading are baseline-subtracted and plotted in time prior to a saccade. The positive and negative pre-saccade errors correspond to CW and CCW stimuli, respectively. C) The magnitude of the saccade-triggering error is dependent on the speed of the bar ($p < 0.001$). D) The inter-saccade intervals (ISI) scale inversely with the speed of the bar ($p < 0.001$). E) The integrated error between saccades changed little as the speed increased ($p=0.261$). Insets for C–E (dotted lines) show how each quantity was evaluated. $n = 2,698$ saccades from 10 animals. See also Figure S2.

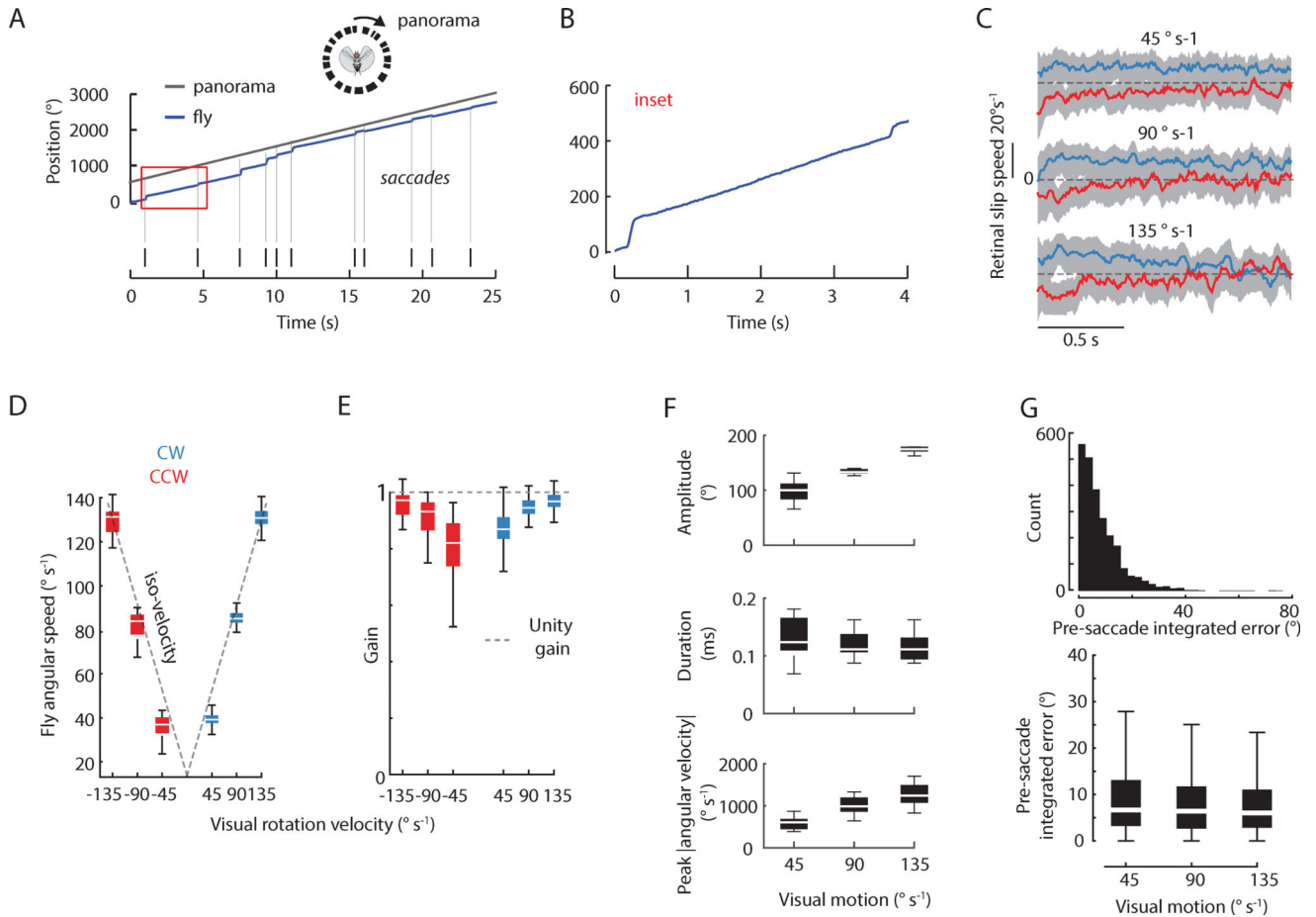


Figure 3. Optomotor saccades are triggered by a threshold in the fixed time integral of velocity
 A) Example 25-second trial of fly tracking the motion of a rotating visual landscape at 90°s^{-1} . Vertical lines represent individual saccades. For visual clarity, the panorama position is offset from 0 deg. B) Inset expanded from red box in panel A to show smooth optomotor movement. C) Mean retinal slip, in units of velocity, during the average 1.5 s interval of smooth movement between saccades across three different rotation speeds for CW (blue) and CCW (red) rotation across all animals. Gray area: SEM. D) Box plot of fly angular velocity with respect to motion of the visual landscape. Gray dashed line: slope of 1 where visual rotation velocity is equal to fly angular speed. E) Same data as panel D but for optomotor gain (fly speed divided by visual rotation speed) across visual rotation velocities. Gray dashed line = unity gain. F) Saccade dynamics across three speeds of panorama motion. Speed had a significant effect on dynamics ($p < 0.001$ for all). G) Top: Distribution of pre-saccade integrated error for all speeds pooled. Bottom: Pre-saccade integrated error is speed invariant. For all panels: 2,232 saccades during optomotor response for CW and CCW rotation, $n = 10$ flies, 451 trials. See also Figure S3 and and Movie S2.

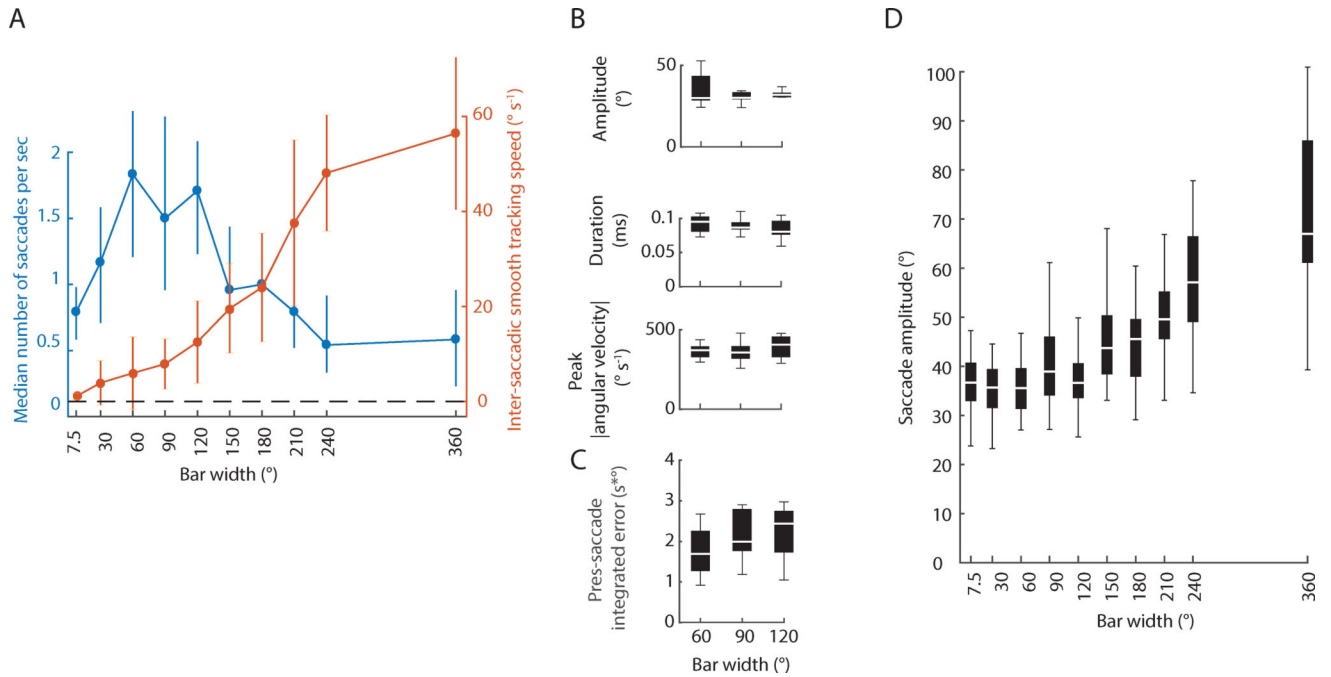


Figure 4. Bar width does not influence saccade dynamics or pre-saccade integrated error

A) Switch between saccade and smooth movement as a function of bar width. Blue circles: median; error bars: 25th–75th percentile. Orange error bars: mean \pm STD. $n = 40$ animals, 1380 trials, 32,802 saccades. Speed = $\pm 75^\circ \text{ s}^{-1}$. B) Saccade amplitude, duration and peak angular velocity is not influenced by bar width. C) Similarly, the pre-saccade integrated error varies little as the bar width increases. Bar velocity = $\pm 75^\circ \text{ s}^{-1}$. $n = 10$ animals, 2,575 bar-fixation saccades. D) Saccade amplitude across the full range of bar width tested. Bar velocity = $\pm 75^\circ \text{ s}^{-1}$. $n = 10$ animals, 10,067 saccades. See also Figure S4.

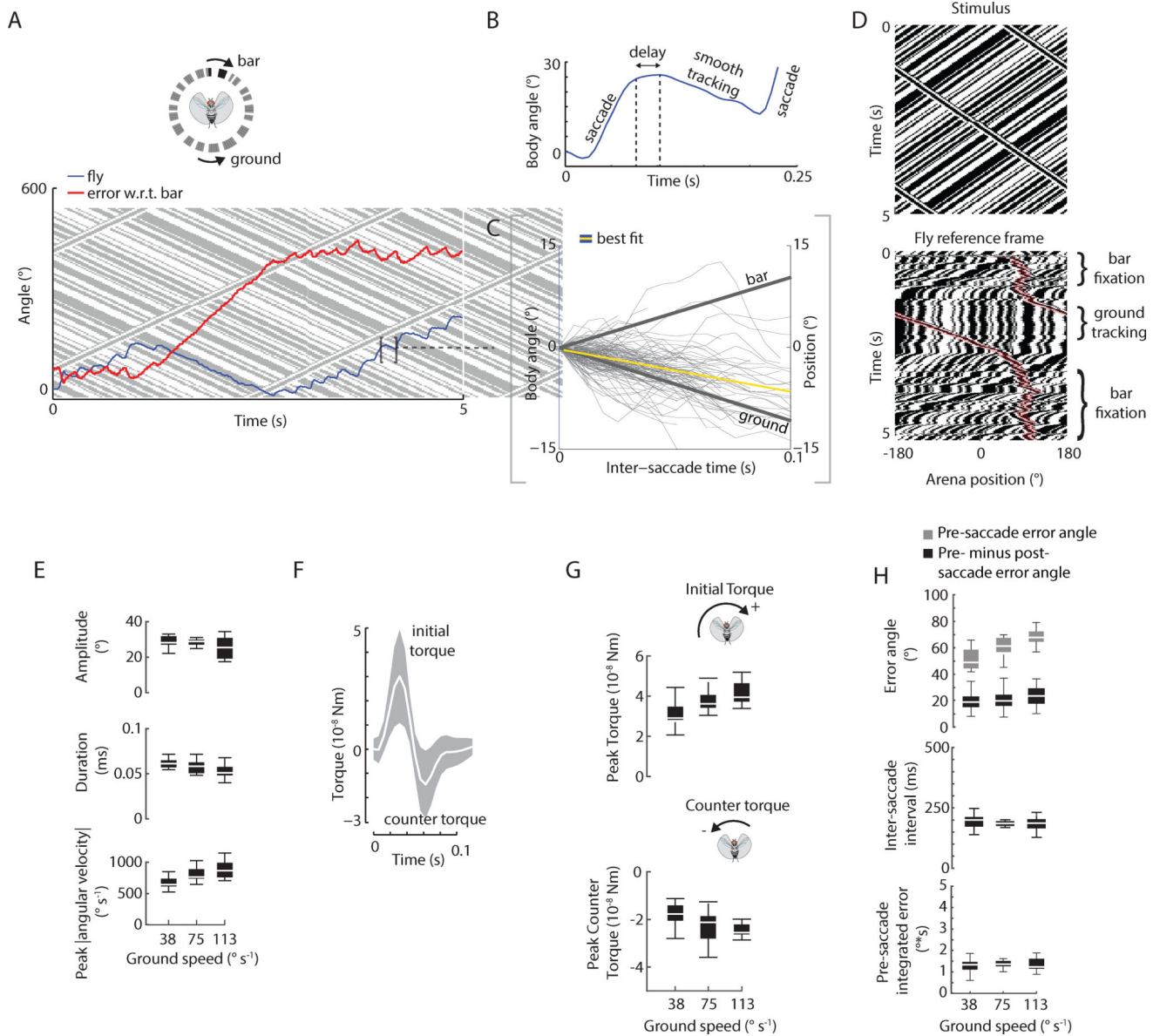


Figure 5. Flies use body saccades to track a bar on a counter-rotating background, quickly switching to smooth movement between saccades, and saccades dynamics, but not saccade-triggering error angle, are influenced by ground speed

A) The compound stimulus is depicted by a space-time diagram in shaded gray as in Figure 1D. Fly heading (blue) and error angle (red) between the fly and the bar. The fly switches between saccadic bar fixation and smooth movement. Note that the fly's body angle lags behind the bar. B) Expanded view of the trajectory if a single saccade indicates rapid transitions between a bar pursuit saccade and smooth tracking of the ground. Median delay = 25 ms. C) Flies track the ground between saccades. Body angle (blue) is baseline-subtracted to show the time course of body angle between saccades during a bout of bar fixation. The yellow line denotes the best-fit line of the body angle data. $n = 1,361$ saccades from 10 animals. D) Top: space-time graph of task shown in A with bar and background revolving in opposite directions. Bottom: space-time graph in the fly's reference frame showing rapid

switching between saccades and smooth movement. The bar is highlighted in pink for visual comparison. E) Ground velocity has subtle but significant effect on saccade duration, amplitude, and peak angular velocity. F) Flies generate an initial torque followed by a counter torque. The black line shows the mean torque. Shaded areas are ± 1 STD. G) Initial peak torques and counter-torques are tuned to the ground speed. H) The error scales with ground speed and marginally for ISI whereas integrated error does not change. $n = 1,361$ saccades from 10 animals. See also Figure S5 and Movie S3.

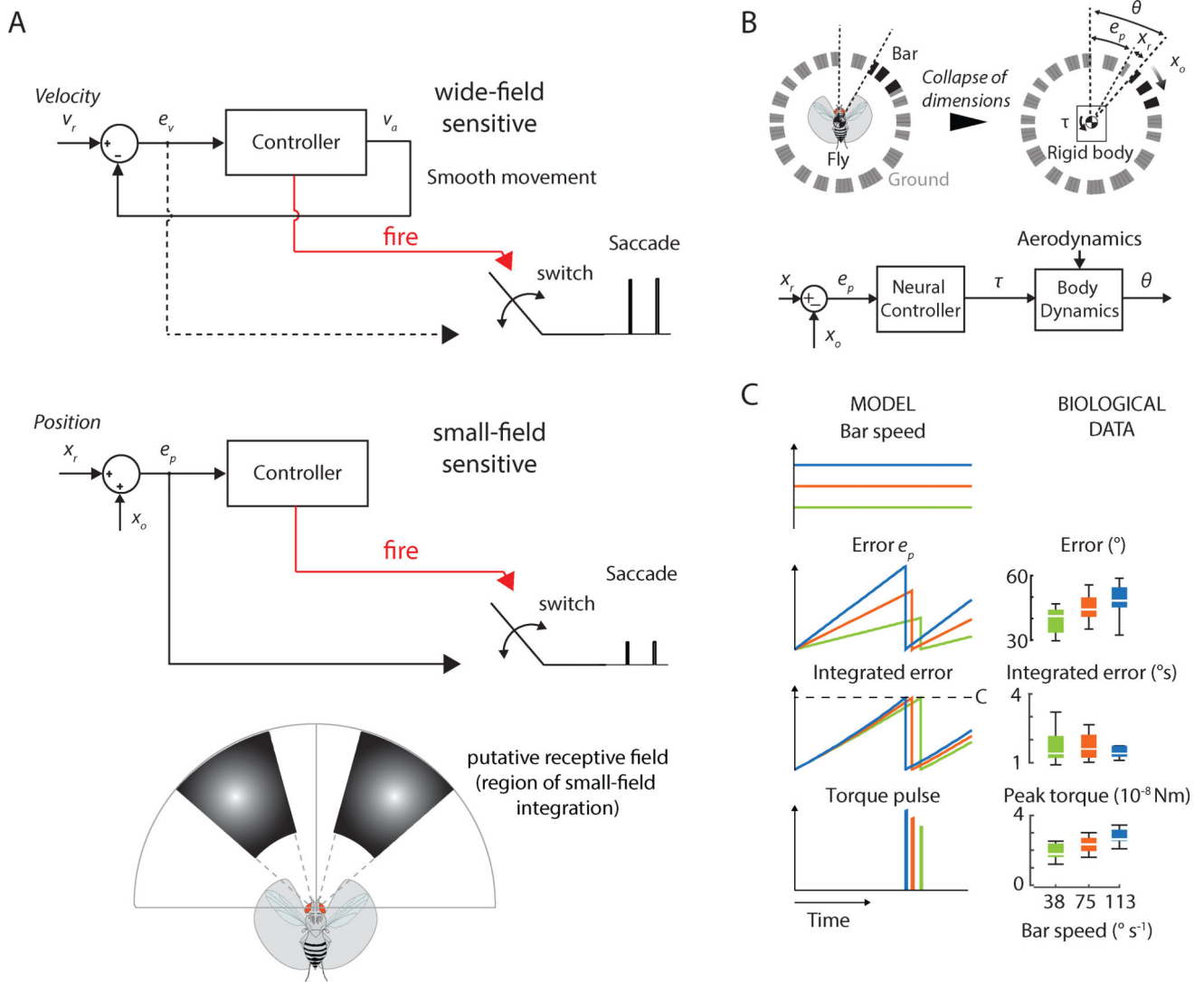


Figure 6. A switched, integrate-and-fire model simulates saccade control

A) A parsimonious model of saccade control suggests parallel position and velocity controllers. Top: The velocity controller drives smooth movement and saccades whereas the position controller drives only saccades (bottom). Red lines: command (fire) signal when integrated error reaches a set threshold. The command signal triggers a change in switch state allowing the error to flow to generate appropriately scaled saccades. While not demonstrated explicitly, for the wide-field sensitive system we hypothesized that e_v scales with motion speed to provide the appropriate tuning of saccades. v_r : reference velocity; e_v : retinal slip error; v_a : actual fly velocity; x_r : reference position; e_p : position error; x_o : bar position. For the position controller, our data suggest a narrow, bilateral receptive field for integration of bar position. B) To determine whether a simple mechanism could simultaneously capture the constant-threshold saccade trigger and the tuning of control torque dependent on bar speed, we constructed a reduced-order, switched control model of bar fixation via a position controller. C) Error, integrated error and torque pulse amplitude generated for three simulated bar speeds (blue, green, red lines). The integrate-and-fire

model fires when the integrated error reaches a constant threshold (C ; Figure S6). The behavioral data is shown on the right for comparison. See also Figure S6.

Author Manuscript

Author Manuscript

Author Manuscript

Author Manuscript